NASA Technical Memorandum 107425

An Experimental Study of the Effect of Wake Passing on Turbine Blade Film Cooling

James D. Heidmann and Barbara L. Lucci
Lewis Research Center
Cleveland, Ohio

Eli Reshotko
Case Western Reserve University
Cleveland, Ohio

Prepared for the
42nd Turbo Expo
sponsored by the American Society of Mechanical Engineers
June 2–5, Orlando, Florida, 1997

National Aeronautics and
Space Administration

AN EXPERIMENTAL STUDY OF THE EFFECT OF WAKE PASSING ON TURBINE BLADE FILM COOLING

James D. Heidmann
Barbara L. Lucci
NASA Lewis Research Center
Cleveland, Ohio

Eli Reshotko
Case Western Reserve University
Department of Mechanical and Aerospace Engineering
Cleveland, Ohio

ABSTRACT

The effect of wake passing on the showerhead film cooling performance of a turbine blade has been investigated experimentally. The experiments were performed in an annular turbine cascade with an upstream rotating row of cylindrical rods. Nickel thin-film gauges were used to determine local film effectiveness and Nusselt number values for various injectants, blowing ratios, and Strouhal numbers. Results indicated a reduction in film effectiveness with increasing Strouhal number, as well as the expected increase in film effectiveness with blowing ratio. An equation was developed to correlate the span-average film effectiveness data. The primary effect of wake unsteadiness was found to be correlated by a streamwise-constant decrement of $0.094 \cdot St$. Steady computations were found to be in excellent agreement with experimental Nusselt numbers, but to overpredict experimental film effectiveness values. This is likely due to the inability to match actual hole exit velocity profiles and the absence of a credible turbulence model for film cooling.

NOMENCLATURE

C	model coefficient
c	blade chord
D	cylindrical rod diameter
d	cooling hole diameter
h	heat transfer coefficient
k	thermal conductivity
L	cooling hole length
M	blowing ratio
N	rotor speed in rpm
n	number of rods in rotor
Nu	Nusselt number
q"	heat flux per unit area
S	effective slot width
St	Strouhal number
T	temperature
V	velocity
x	streamwise distance from leading edge
y^+	dimensionless distance from wall
η	film effectiveness
ρ	density

Subscripts

c	coolant conditions
f	film conditions
r	recovery conditions
w	wall conditions with heating
∞	freestream conditions

INTRODUCTION

As a result of efforts to improve turbine engine performance, turbine inlet temperatures have increased dramatically over the past 50 years. Current turbine inlet temperatures are approaching 2000 K, while the best available metallic turbine materials can withstand a maximum temperature of only about 1300 K. When internal cooling alone is inadequate, film cooling must be employed. In film cooling, the coolant air is discharged through small holes in the turbine surface to form a protective film between the turbine blade and the hot combustor discharge gas.

The flow in turbomachinery blade rows is inherently unsteady due to the relative motion of adjacent blade rows. Wake passing from upstream blade rows causes periodic fluctuations in the magnitude and relative direction of the flow velocity in downstream blade rows. Precisely modeling a turbomachinery flow field thus requires inclusion of the time-varying quantities. However, due to the complexity of the unsteady flow field, the design of turbine film cooling schemes has tended to rely on steady databases.

Because of its importance in turbine design, there has been much investigation into the behavior of turbine film cooling flows. Goldstein (1971) reviewed the early research in the film cooling arena. This

review consolidated flat plate experiments of various hole geometries and blowing parameters, and summarized analytical solutions for two-dimensional slot injection. The experimental studies typically had long film holes (L/d greater than 10.0). More recent steady film cooling research is summarized by Heidmann (1996). The more recent studies generally consider L/d values more typical of turbine blades (between 2.0 and 4.0), as well as actual blade profiles.

Relatively less work has been done on the impact of unsteadiness on film cooling in a turbine blade. Rigby et al. (1990) used a rotating wheel wake generator with cylindrical bars to model inlet guide vane wakes and shock waves under transonic flow conditions. The test blade was film cooled on both the suction and pressure sides. The main effect of the wake passing was a reduction in effectiveness caused by enhanced film mixing, and the shock passing effect was found to produce large fluctuations in the heat transfer rate. Ou et al. (1994) and Mehendale et al. (1994) used an experimental approach similar to Rigby et al (1990), except with a different blade profile, subsonic flow, and including showerhead cooling. Both air and CO_2 injection were employed for different density ratios. Ou et al. (1994) found that increasing wake passing frequency increases local Nusselt numbers for all blowing ratios, but this effect is reduced at higher blowing ratios. Mehendale et al. (1994) found that an increase in wake passing frequency causes a decrease in film effectiveness over most of the blade surface for all cases considered. Funazaki et al. (1996) used a rotating wheel wake generator with cylindrical bars upstream of a showerhead-cooled blunt body. Heated air was used as the injectant. Increasing wake passing frequency was found to reduce film effectiveness, especially at lower blowing ratios where the influence of the wake on the low momentum film is strongest. The wake effect was reduced as free-stream turbulence increased.

Several studies have investigated film cooling performance on a turbine blade in an actual rotating turbine stage environment. Dring et al. (1980) studied film cooling performance on a large scale model of a high pressure turbine first stage. Coolant was injected from a single hole on both the pressure and suction sides of the rotor blade. Density ratios from 1.0 to 4.0 were investigated and flow visualization studies showed radial migration of the coolant, especially on the pressure side. The migration was found to be relatively insensitive to the coolant properties. Film effectiveness profiles were measured downstream of the holes. The suction surface profiles were found to correlate well with flat plate data, while the pressure surface film effectiveness was significantly reduced. Takeishi et al. (1992) also measured film cooling effectiveness for a rotating turbine blade. In this case, the blade had a realistic cooling geometry with showerhead, pressure, and suction surface rows of cooling holes. The results of Dring et al. (1980) were corroborated, as the pressure surface film effectiveness was found to decrease relative to cascade tests due to the radial flow and concave curvature. The suction surface film effectiveness was in good agreement with the stationary blade tests except far downstream where enhanced mixing reduced the film effectiveness. Abhari and Epstein (1992) used a short duration turbine test facility to again study a film-cooled rotating blade in a turbine stage environment. The cooling arrangement consisted of three rows of coolant holes on the pressure surface and two on the suction surface, but no showerhead cooling. Unlike Dring et al. (1980) and Takeishi et al. (1992), this study considered transonic flow. This introduced unsteady shock passing in addition to wake passing as unsteady effects. For these tests, the suction surface had a 12 percent decrease in heat transfer, while the pressure surface had a 5 percent increase relative to cascade tests. The unsteady effects were attributed to coolant flow rate changes caused primarily by shock passing pressure fluctuations.

Unsteady numerical simulations for an entire film-cooled turbine stage are scarce due to the large computational time associated with capturing both the small time scales of blade passing and the small length scales of film cooling and heat transfer. However, Dorney and Davis (1992) showed that such a simulation could be achieved using a time-accurate Navier-Stokes solver. The computational constraints limited the simulation to only two grid points per film hole, so local effects due to hole exit profile could not be modeled.

Although recent research has begun to focus on the unsteady flow environment, the majority of research on film coolant flow has considered the turbine free stream flow to be steady. Studies of film cooled turbine stages include unsteadiness, but lack the ability to vary the unsteady parameter. Cylindrical wake experiments solve this problem, but have not sought to resolve spanwise and time variations to isolate the important physical phenomena associated with film coolant flow. The present study aims to investigate the effect of flow unsteadiness on turbine film cooling in a more detailed and fundamental manner. Showerhead cooling is chosen because of the larger temporal fluctuations in static pressure in the leading edge region and the effect of incidence on showerhead cooling behavior.

EXPERIMENTAL APPARATUS AND PROCEDURE

The experiment was conducted in the NASA Lewis Rotor-Wake Heat Transfer Rig. This annular-flow open-circuit wind tunnel was described in detail by Simoneau et al. (1984). The facility has a rotor upstream of the test section (Fig. 1) which is capable of rotating at speeds up to 7000 rpm. The rotor has 24 equally spaced 3.2 mm diameter cylindrical rods at 15° intervals. O'Brien and Capp (1989) described the two-component phase-average turbulence statistics

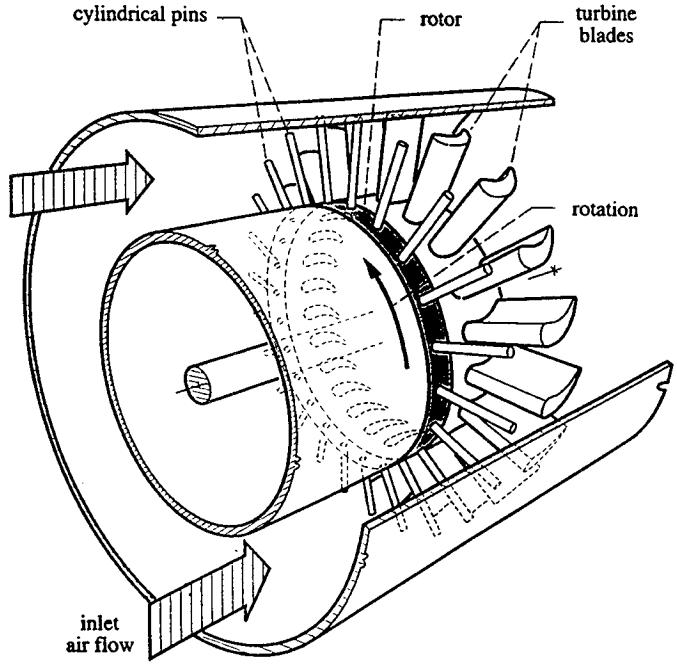

Figure 1: Rotor-wake facility schematic.

downstream of the rods. Cylinder wakes cannot model the boundary layer and loading of an upstream blade. However, the velocity deficit, turbulence production, and rotative speed are all modeled to some degree. Downstream of the rotor is an annular turbine cascade consisting of 23 turbine blades with 67° of turning. The blade profile is shown in Fig. 2. Since the nominal inlet flow direction is axial, blades in the cascade have an inlet angle of 0° for optimum incidence. All tests were conducted at a cascade inlet Mach number of 0.27. This corresponds to a blade Reynolds number of about 4.0×10^5 based on blade chord.

A secondary flow supply system was developed to allow injection of film cooling flow through the test blade. This system was designed to supply both air and CO_2 to the test blade. CO_2 has a molecular weight of 44.01 compared to 28.97 for air, so at the same pressure and temperature, it has a density 1.519 times that of air. This allows more realistic density ratios to be achieved in the experiment. In order to measure thermal film effectiveness values, the secondary flow must be at a different temperature than the free-stream. To heat the secondary flow in the test facility, an electrical resistance heater was employed. For air and CO_2, this heater provided secondary flow temperature rises of about 35 K and 30 K, respectively, owing to differences in specific heat for the two gases. The secondary flow temperature and pressure were measured by a thermocouple and static tap, respectively, centered in an upstream plenum.

The test blade was assembled in several parts, as shown in Fig. 2. The bulk of the blade is wood, which was used because of its low thermal conductivity to reduce thermal conduction in the blade. In order to allow determination of heat transfer coefficients on the blade

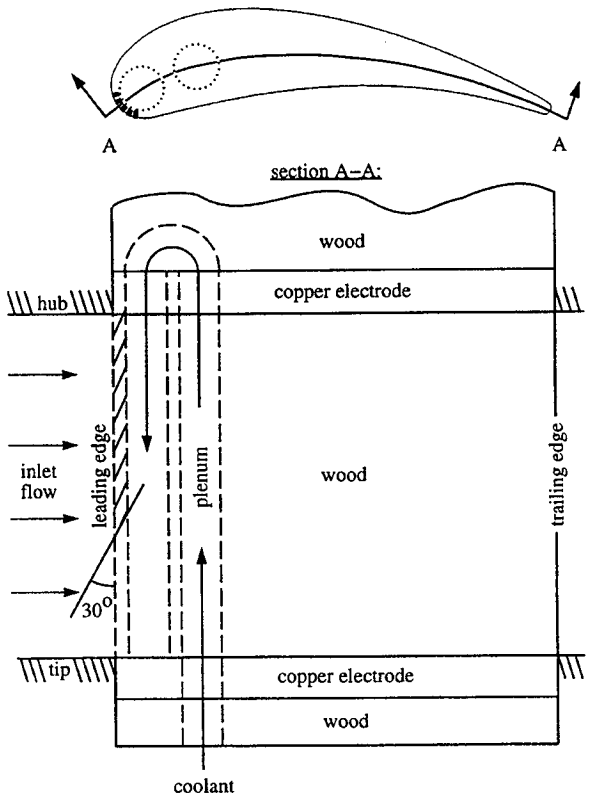

Figure 2: Blade geometry.

surface, a heat source is required. A 0.025 mm thick sheet of Inconel foil was used as a resistive heater. A rectangular sheet of the foil was used to cover both the suction and pressure surfaces of the blade, leaving the showerhead region exposed. Two copper electrodes were machined having the same profile as the blade, and a thickness of 6.3 mm. These electrodes were glued into the test blade. The foil was attached to both electrodes using a continuous line of very small spot welds to assure a uniform distribution of heat flux over the blade surface. A circuit current of 36 Amperes was used in the experiment. This current was determined to be sufficient to generate a nominal temperature increase of 10 K on the blade surface under standard flow conditions.

The secondary flow passage as shown in Fig. 2 is a 6.3 mm diameter hole which extends the length of the rig annulus to the inner diameter, makes a 180° turn, and extends back toward the outer diameter. The film cooling hole pattern is presented in Fig. 3, and consists of five staggered rows of 1.0 mm diameter showerhead film holes. The holes are angled at 30° to the surface in the spanwise direction and are oriented toward the outer diameter. The holes are 3.5 mm long, resulting in a length-to-diameter ratio (L/d) of 3.5. The pitch-to-diameter ratio in both the spanwise and streamwise directions is 4.0. There are 17 holes in rows 1, 3, and 5, and 16 holes in rows 2 and 4. In order to establish a more periodic flow in the midspan region of the blade, holes 11 through 17 in all rows were permanently covered with smooth tape. Computations by Heidmann (1995) using the viscous flow solver rvc3d (Chima and Yokota, 1990) were used to place the holes such that the flow from the center row would evenly split between the suction and pressure sides.

The test blade was instrumented with an array of 72 nickel thin-film gauges. The gauges were manufactured by Tao Systems, Inc., and consist of serpentine nickel sensing elements with copper leads. To allow spanwise resolution of the temperature profile behind the film cooling hole pattern, eight gauges were placed near midspan at each of nine streamwise locations, five on the suction side and four on the pressure side. These eight gauges were situated to completely span one unit cell of the hole pattern as shown in Fig. 3. The streamwise length of each gauge is 1.0 mm. The first row on each surface is 8.0 mm downstream of the center row of film holes, and the subsequent rows are spaced at 13.5 mm intervals. Pressure surface distances are considered positive. The thin-film gauges were calibrated by the Cortez III Service Corporation. The steady data recording system reads the gauge signals once per second for twenty seconds and records the average value of all data. The amplified AC component of the gauge signals are recorded on the Masscomp data system at a frequency necessary to record about 50 time steps per wake passing. The signals are recorded for a period of about 1200 wake passings. The unsteady data are then phase-averaged.

The experiment was conducted for blowing ratios of 0.5 and 1.0. The definition of blowing ratio used to determine the required injectant velocity is:

$$M = \frac{\rho_c V_c}{\rho_\infty V_\infty} \qquad (1)$$

where c indicates injectant conditions and ∞ indicates freestream conditions. The ratio of injectant to freestream density for air and CO_2

was 0.90 and 1.38, respectively. The experiment was conducted for Strouhal numbers of 0.167, 0.250, 0.500, and 0.600. The definition of Strouhal number used to determine the required rotor speed is:

$$St = \frac{2\pi NDn}{60V_\infty} \quad (2)$$

where N is the rotor speed in rpm, D is the cylindrical rod diameter, n is the number of rods in the rotor, and V_∞ is the cascade inlet axial velocity. Baseline steady cases for comparison to the rotating data were established by two different methods. In the first method, eight test cases were investigated with the rotor fixed in eight equispaced positions relative to the test blade. The results from these cases were averaged for comparison to the rotating cases. An alternative baseline case was established with no upstream rotor.

The definition of film effectiveness for compressible flow is:

$$\eta = \frac{T_f - T_r}{T_c - T_r} \quad (3)$$

where T_f is the film temperature, T_r is the recovery temperature, and T_c is the injectant stagnation temperature. Film temperatures were measured in the presence of film injection under an adiabatic wall condition. Recovery temperatures were determined from tests with thin tape over the film holes without heating the blade. Radiation errors were estimated to be approximately offset by backside heating due to the warm plenum. The definition of heat transfer coefficient is:

$$h = \frac{q''}{T_w - T_f} \quad (4)$$

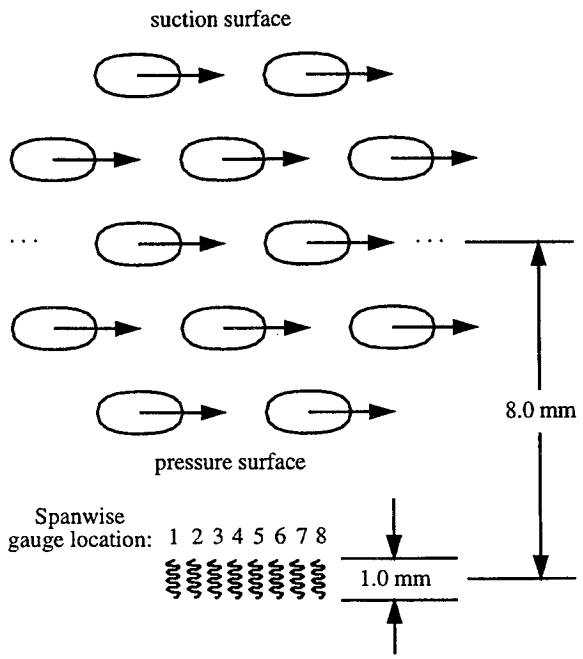

Figure 3: Film hole and gauge arrangement.

where T_f is the film temperature as measured in Eq. (3) and T_w is the wall temperature with film cooling and a local heat flux of q". The errors in q" due to radiation and conduction are now complementary, but their magnitudes are small since only differences between the adiabatic wall and heated wall cases are important. The maximum error in q" due to these effects is approximately 1.0%, which is well within the experimental accuracy. The Nusselt number is defined as:

$$Nu = \frac{hc}{k} \quad (5)$$

where c is the blade chord length (63.5 mm), and k is the thermal conductivity of the film. For air injection, a constant thermal conductivity is used. For CO_2 injection, a mixture of gases is present at the wall, and the procedure of Bird et al. (1960) is used to estimate the thermal conductivity at the wall.

EXPERIMENTAL RESULTS

Figure 4 shows the steady span-average film-effectiveness versus streamwise distance for the four blowing conditions. The symbols indicate experimental data and the curves represent the correlating equation to be discussed in the following section. The no rotor case is with the rotor removed and no wakes present. The St=0, ave. case is the average of the eight equispaced stationary rotor test cases. Each case has an incrementally varying wake location relative to the blade, spanning one circumferential pitch of the rotor rods. Although the Strouhal number is thus zero for this case, the effect of the wake is apparent as a reduction in film effectiveness relative to the no rotor case. All four plots indicate a general reduction in film effectiveness as the level of unsteadiness increases. This reduction is nearly monotonic with increasing Strouhal number, and may be explained by the increased mixing which dissipates the film layer. The reductions in film effectiveness are most pronounced on the blade suction surface. This phenomenon is explained by the swirl caused by the rotor. For the no rotor and stationary rotor cases, no swirl is imparted to the flow by the rotor, and the flow enters the cascade with zero swirl. This condition establishes a particular attachment line on the blade, and determines the split of coolant between the suction and pressure sides of the blade. As the Strouhal number increases, the wake-producing rods impart swirl to the freestream toward the pressure side of the blade. This moves the attachment line toward the suction side, and skews the coolant flow toward the pressure side of the blade. This in turn increases the film effectiveness on the pressure side compared to the suction side. However, this effect is smaller than the reduction due to increased mixing, so the overall effect of increased Strouhal number is to reduce film effectiveness on both the suction and pressure sides of the blade. For both injectants, the M=1.0 case provides higher film effectiveness than the M=0.5 case, indicating that the film remains attached to the blade surface at M=1.0. This is due to the relatively shallow angle of injection and the very nature of showerhead cooling. The freestream velocity is nearly normal to the blade surface, which tends to force the injectant to remain attached. Nusselt numbers are found to remain nearly constant under changes in Stouhal number.

Figure 5 presents the M=1.0 no rotor experimental film effectiveness data in comparison with calculations performed using the viscous flow solver rvc3d with no upstream wake. The computational

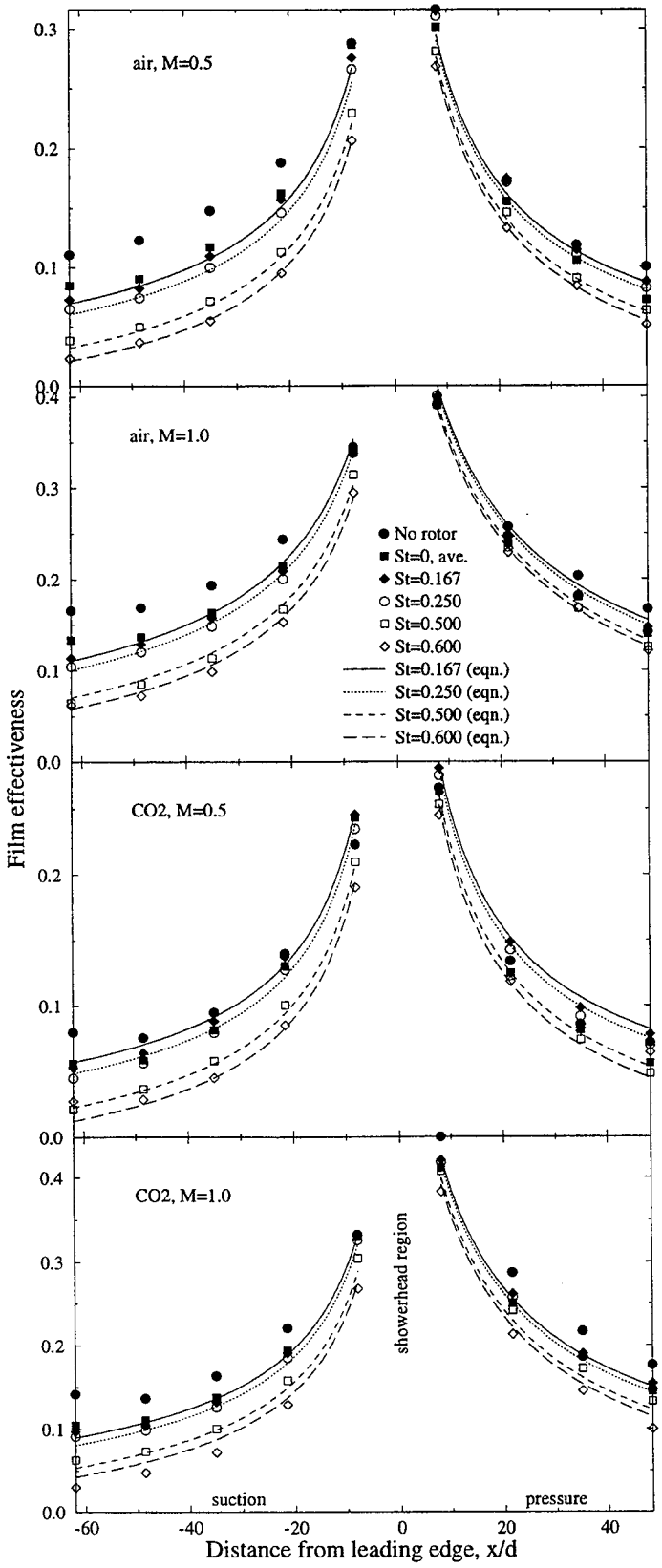

Figure 4: Time- and span-average film effectiveness.

method is described in detail by Heidmann (1995). The present computations were performed using a 305x90x20 grid with a y^+ value of less than 1.0 at the first grid point from the wall and with the Baldwin-Lomax turbulence model. Three different injectant conditions were computed: CO_2 injection at an angle of 30°, CO_2 injection at 45°, and air injection at 30°. All cases are for M=1.0. Since the code cannot model multiple species, CO_2 injection was modeled using a reduced injection temperature to match the experimental density ratio. All three computations overpredict the experimental film effectiveness, particularly on the downstream suction surface. Since the blowing ratio and hole area are matched, this must be due to an underprediction of film mixing by the computation. This may result from not resolving the flow inside the film holes as well as the lack of an accurate turbulence model for film cooling. The injectant temperature has a moderate effect on the film effectiveness. Decreasing the injectant temperature to model CO_2 decreases the film effectiveness on the pressure surface and increases it on the near suction surface. This is in contrast to the trend exhibited by the experimental data, where the air performs better on the suction surface but worse on the pressure surface. This may be due to species differences which the computer code is unable to model. The effect of increasing the injection angle from 30° to 45° is negligible on the suction surface and causes a slight decrease in film effectiveness on the pressure surface. However, very near the showerhead region the more normal injection performs markedly better. On the pressure surface, the 45° injection provides a better film to an x/d value of about 10, at which point the enhanced mixing caused by the more normal injection predominates and lowers the effectiveness.

Figure 6 shows the Nusselt number distributions for the same conditions as Fig. 5. The computations are in very good agreement with the experimental data, particularly on the suction surface. The effect of changing the hole angle is small, while CO_2 injection produces higher Nusselt numbers than air injection by a nearly constant offset of about 350. This trend is remarkably consistent with the experimental data, which also shows increased Nusselt numbers for CO_2 injection. These increases are likely due to density ratio differences rather than species differences since the code cannot model species differences.

Span-resolved data were recorded for all wake and blowing cases. Except for the x/d=-8.0 location, the film effectiveness distribution is

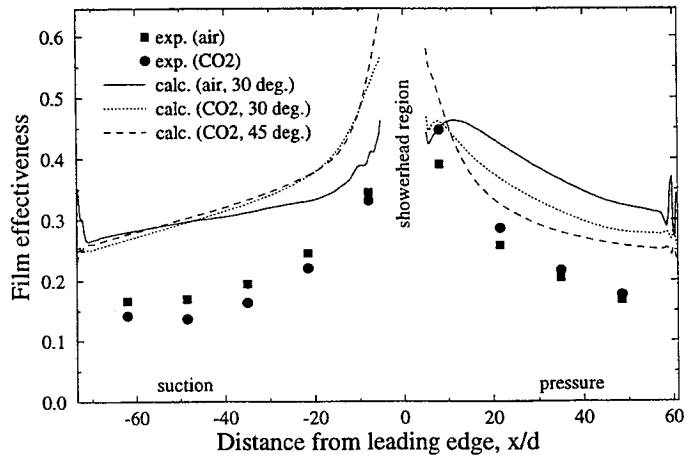

Figure 5: Steady span-average film effectiveness, M=1.0.

nearly uniform. At x/d=-8.0 (Fig. 7), a large spanwise variation in film effectiveness is found. Spanwise gauge location 1 is repeated as location 9 to complete one spanwise unit cell. Data points are only shown for working gauges. The trends are consistent for all Strouhal number cases. The largest spanwise variations occur when the rotor is removed, due to the absence of wake-induced mixing of the film. As the Strouhal number is increased, not only does the span-average film effectiveness decrease, but the spanwise variations decrease as well, indicating that the higher wake passing speeds provide more spanwise mixing of the film. Spanwise locations 2 and 3 comprise the lowest film effectiveness region, and thus correspond to the gap between two adjacent film jets. It appears that the presence of a rotor wake actually increases the film effectiveness slightly in this region. This increase offsets the decrease in the high film effectiveness region (spanwise locations 5 through 8), so the span-average film effectiveness is not degraded by the presence of a rotor wake or by increasing Strouhal number up to about St=0.250. This helps explain the behavior seen in on the suction side in Fig. 4, where the presence of a rotor has a greater effect at larger distances from the film holes. Near the film holes, the wake acts to effectively spread the film jet, reducing spanwise gradients but not the span-average film effectiveness since the gaps between the film jets are filled. Farther downstream, the effect of this spanwise mixing of the jet begins to reduce the span-average film effectiveness since the low film effectiveness gaps are already filled, and no additional benefit results from spanwise mixing. Nusselt number results indicate very little spanwise variation, even near the leading edge.

The gauges showed some time variations of film effectiveness, but these were random and lacked repeatability. The attempts to extract meaningful unsteady results are documented in detail by Heidmann (1996). Conduction effects in the substrate were the primary cause of this problem. Because of these difficulties, it was decided to scrutinize the results from the stationary wake data that was obtained as a limiting case of zero Strouhal number. Figure 8 shows the span-average steady film effectiveness variations with rotor wake location for the suction and pressure surfaces of the blade. Wake location 5 is for the wake aligned with the blade leading edge. Wake location 1 is the same as location 9, and is for the wake at mid-passage. These plots represent the limiting case of the rotating tests at zero rotational speed.

The suction surface results show a highly repeatable distribution for all streamwise locations. With the wake impinging on the blade (wake location 5), the film effectiveness is reduced by about 0.05 at x/d=-8.0 and almost 0.10 at the downstream locations. This result is expected due to the enhanced film mixing caused by the increased turbulence in the wake. It is surprising that the absolute reductions in film effectiveness are greater at the downstream locations, because the levels of film effectiveness are lower at these locations. However, this supports the explanation given for the behavior in Fig. 7. The impingement of the wake on the leading edge increases spanwise

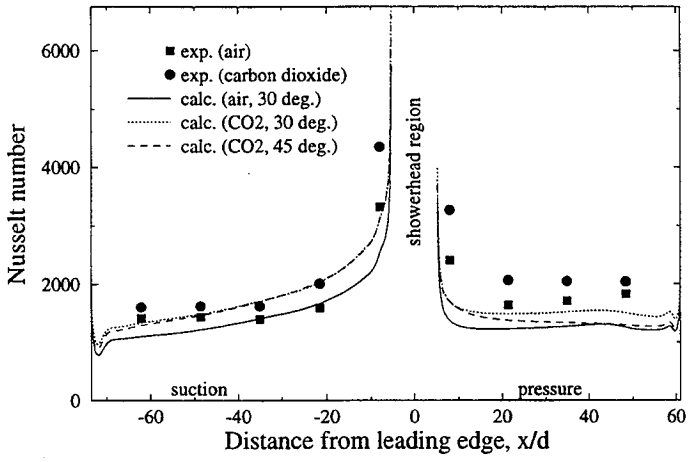

Figure 6: Steady span-average Nusselt number, M=1.0.

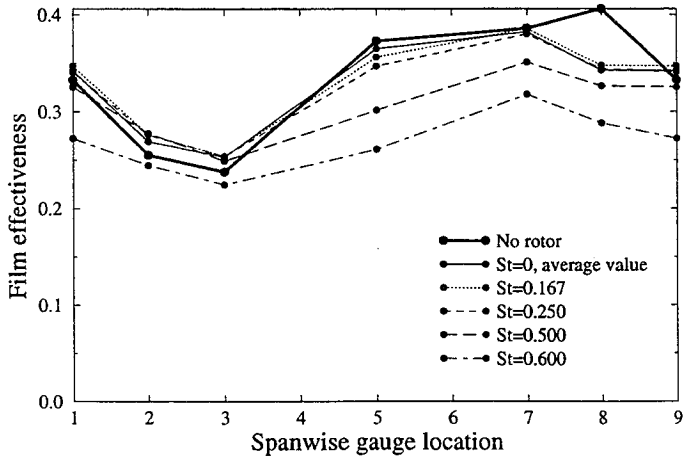

Figure 7: Local film effectiveness, CO_2, M=1.0, x/d=-8.0.

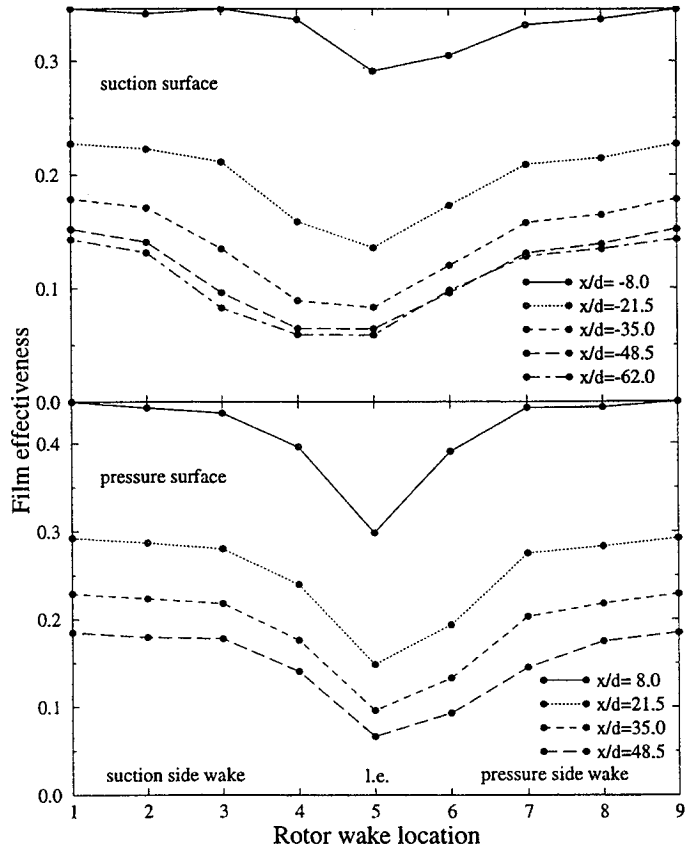

Figure 8: Span-average film effectiveness, CO_2, M=1.0, St=0.

mixing of the film, but this action is actually favorable in the low effectiveness gaps between jets, which at x/d=-8.0 partially offsets the detrimental dissipation of the film. The pressure surface results indicate an even greater reduction in film effectiveness due to wake impingement than on the suction surface. Reductions of about 0.15 at x/d=8.0 and at least 0.10 downstream are noted. Both the suction and pressure surface data show an asymmetry of the film effectiveness profile. For both sides of the blade, the film effectiveness is reduced more for a wake location nearer that side, as expected. Thus the suction surface film effectiveness is reduced more at wake locations 3 and 4 than at wake locations 6 and 7, while the opposite is true on the pressure surface. The only streamwise location which indicates an effect of wake location on Nusselt number is at x/d=8.0, which is the pressure surface leading edge. The wake exhibits a velocity defect which decreases the Nusselt number by about 20 percent because of lower velocity gradients at the wall.

WAKE-AFFECTED FILM COOLING MODEL

Analytical film effectiveness correlations for slot injection are given by Goldstein (1971), and are typically of the form:

$$\eta = \frac{C_1}{1.0 + C_2\left(\frac{x}{MS}\right)^{C_3}} \qquad (6)$$

where C_1, C_2, and C_3 are constants, x is the streamwise distance from the slot, M is the blowing ratio, and S is the slot width. For film cooling on a blade with discrete holes, an analytical description of the boundary layer is usually not available. For this case, empirical correlations are often used, although their applicability is limited to the geometry and conditions from which they were derived. Using the basic form given for slot injection, others have produced correlations of experimental data. For example, Takeishi et al. (1990) have given an empirical correlation for film effectiveness on a low aspect ratio turbine nozzle with suction and pressure side circular hole film cooling. S now becomes the effective slot width, or the width of a slot having the same flow area as the hole pattern. For n rows of circular holes, $S=n\pi d^2/4p$, where p is the hole spanwise pitch.

The form of the correlation which proved to provide the best agreement with the experimental data for the present experiment is:

$$\eta = \frac{C_1}{1.0 + \left(\frac{C_2 x}{MS(1.0 \pm C_3 M \pm C_4 St)}\right)^{C_5 \pm C_6}} - C_7 St \qquad (7)$$

Positive signs are taken for the pressure surface and negative for the suction surface. S is taken to be half of the effective slot width for all rows of holes. The form of Eq. (7) follows that of Eq. (6), but supplements it with additional terms to account specifically for suction/pressure surface and Strouhal number differences.

The primary effect of the wake unsteadiness on the film effectiveness is to reduce it as the rotational speed or Strouhal number increases. This is evident in Fig. 4. In addition, the change in film effectiveness for a given change in Strouhal number is fairly constant with downstream distance x on either the suction or pressure surface. The $-C_7St$ term is used to model this effect. This term provides excellent agreement over the range of experimental data. In addition, the simplicity of this term allows for ease of interpretation. C_7 is the slope of the film effectiveness versus Strouhal number trend.

The Strouhal number effect, although nearly constant with x, differs on the suction and pressure surfaces due to the shifting of the attachment line. This phenomena is addressed in the correlation through the C_4St term. This term arises from an assumption that the changes in injectant split are linear with Strouhal number. The quantity MS is an effective flow rate and is modified in the correlation to be $MS(1.0\pm C_3M\pm C_4St)$. This modification maintains the total flow rate on both sides of the blade at 2MS.

The term C_3M arises from the observation that the difference between the pressure and suction surface film effectiveness is greater for M=1.0 than for M=0.5 for both air and CO_2 injection. The physical interpretation of the C_3M term is that the injectant split depends upon the blowing ratio. At low blowing ratios, the momentum of the injectant is low, and the split between pressure and suction surfaces depends primarily on the geometric location of the film holes. At high blowing ratios, the injectant penetrates more deeply into the freestream, and the split may be influenced by the angle of injection and freestream flow behavior. For the present experiment, the pressure surface is favored for higher blowing ratios, but this may be due to geometric considerations unique to this configuration.

The C_6 term represents the fact that the film effectiveness was found to decay more rapidly in the streamwise direction on the pressure surface than on the suction surface. This finding agrees with the analysis of Ito et al. (1978), which predicts better film cooling performance on a convex wall than on a concave wall for streamwise momentum flux ratios less than 1.0. For the showerhead cooling of the present experiment, the injectant exits the hole with zero streamwise momentum, resulting in a streamwise momentum ratio of zero for all cases. Thus the convex (suction) surface should perform better than the concave (pressure) surface to the same degree for all blowing cases. The experimental data agrees with this prediction. Additionally, the analysis of Ito et al. (1978) pertains to the performance of a fluid element once it has established a trajectory on either side of the blade. Because of this the C_6 term should be independent of blowing ratio for showerhead cooling, and is incorporated as such in the exponent.

The application of a least-squares algorithm on the experimental data produced the coefficients for Eq. (7) shown in Table 1.

Table 1: Correlation Coefficients for Equation 7.

	air	CO_2
C_1	0.761	0.948
C_2	0.054	0.094
C_3	0.139	0.241
C_4	0.286	0.144
C_5	0.792	0.762
C_6	0.033	0.014
C_7	0.093	0.095

The root mean square average of the error in film effectiveness using

these coefficients is about 0.0068 for air and 0.0074 for CO_2.

In terms of their effect on the film effectiveness, C_5 and C_7 remain fairly constant between injectants. In particular, the magnitude of the Strouhal number effect (C_7) is almost the same for both injectants, having an average value near 0.094 for both air and CO_2. This may indicate a relative insensitivity of wake passing effects to injectant density ratio. The agreement between C_5 for air and CO_2 indicates that the film effectiveness decay rate is similar for both cases. The fact that the values are below 1.0 implies a more gradual decay of film effectiveness with downstream distance than for the cases of Takeishi et al. (1990), which gave values of 1.0 and 1.6 for a non-showerhead film cooled blade. This is to be expected for showerhead cooling, since the injectant has less opportunity to separate from the blade than does suction and pressure surface injection. C_3, C_4, and C_6 are the three coefficients associated with differences between suction and pressure surface film effectiveness values. All of these coefficients have the same sign for air and CO_2, which indicates that the trend between suction and pressure surface data is consistent for the two injectants. The magnitudes of these coefficients differ, however. It should be noted that the specific heat of CO_2 is 14 percent lower than that of air. As indicated by Mehendale et al. (1994), this causes the measured film effectiveness values for CO_2 to be conservative by up to 14 percent, depending on the concentration of CO_2 at the wall. However, due to the generally small concentrations, this error is estimated to result in less than a 3 percent underprediction of the actual value over most of the blade.

Figure 4 shows comparisons between the experimental data and correlations for air at blowing ratios of 0.5 and 1.0 and CO_2 at blowing ratios of 0.5 and 1.0, respectively. It can be seen that the correlation is in excellent agreement with the experimental data for air injection at both blowing ratios. The change in film effectiveness with increasing Strouhal number is captured quite well. This indicates that the assumption of linear decay of film effectiveness with Strouhal number is proper. In general, the correlation agrees well with the CO_2 data. The magnitude of the Strouhal number effect is underpredicted for a blowing ratio of 1.0, particularly on the suction surface, and is overpredicted for a blowing ratio of 0.5, particularly on the pressure surface. This indicates that the correlation might properly require a blowing ratio influence on the C_7St term. However, in view of the excellent correlation achieved with the relatively simple correlation equation, the recommended correlation stands.

Mehendale et al. (1994) have presented film effectiveness values for St=0.1 and 0.3. Their experiment was conducted for a more highly-loaded turbine blade and consists of suction and pressure surface cooling in addition to the showerhead cooling of the present study, so direct comparisons are difficult. However, the Strouhal number effect is nearly constant in the streamwise direction as in the present study. The mean film effectiveness decrement predicted by the current model for a Strouhal number increase of 0.2 is 0.019. The Mehendale et al. (1994) data set shows a decrement ranging from 0.025 at M=0.8 to slightly negative (enhancement) at M=0.4 on the pressure surface, with a mean value of about 0.013. The model predicts a smaller film effectiveness decrement on the pressure surface due to attachment line variations at higher Strouhal numbers. This effect is present, particularly at M=0.4 and M=1.2, although it is smaller than in the present study, presumably due to the presence of suction and pressure surface (non-showerhead) cooling, which is unaffected by attachment line variations.

CONCLUSIONS AND RECOMMENDATIONS

A model has been developed which accounts for the primary effects of wake passing unsteadiness on film cooling effectiveness for a showerhead-cooled stationary turbine blade. The experimental film effectiveness as correlated by the model is seen to be reduced by wake passing unsteadiness for all cases by a nominal value of 0.094·St. The Strouhal number has a measurable effect on the flow split between the suction and pressure surfaces for showerhead cooling. A higher Strouhal number skews the coolant flow toward the pressure surface, producing better cooling on the pressure surface and worse on the suction surface. Nusselt numbers were found to remain fairly constant with changing Strouhal number, but to be higher for CO_2 than for air injection.

The unsteady experimental data proved difficult to execute and interpret. It is recommended that future experiments which aim to measure high frequency temperature fluctuations use double-sided gauges similar to those used by Abhari and Epstein (1992). Several important mechanisms of wake passing were isolated by other methods. A clear and consistent reduction in film effectiveness was found for stationary wake locations near the blade leading edge. Reductions of up to 0.10 and 0.15 were exhibited on the suction and pressure surfaces, respectively. Nusselt number reductions of about 20 percent were found near the pressure side leading edge with the wake impinging on the blade. Based on the success of these data, stationary wake experiments are recommended in the absence of advanced instrumentation capable of resolving high frequency data. In addition, the averaging of these data more properly represent a limiting case for wake passing experiments than the more traditional no wake condition. Another unsteady mechanism identified by the steady experiments is the spanwise variation in film effectiveness near the suction side leading edge for various Strouhal numbers. The reduction in span-average film effectiveness is found to be primarily due to reductions near the peak film effectiveness value. This indicates that the wake passing influences the film jets by enhancing their spanwise mixing.

Nusselt numbers are predicted quite well by the steady computation. Film effectiveness prediction is not as successful. The computation predicts higher film effectiveness values than the experiments, which indicates an underprediction of film mixing. This is thought to be primarily due to not resolving the flow inside the film holes, as well as the absence of reliable turbulence models for film cooling.

A better understanding of the complex interactions between unsteady flows and film cooling flows is necessary to improve existing models and achieve better film cooling designs It is hoped that the results of this study represent a step in this direction, and will lead to other research in the field.

REFERENCES

Abhari, R. S. and Epstein, A. H., 1992, "An Experimental Study of Film Cooling in a Rotating Transonic Turbine", ASME Paper 92-GT-201.

Bird, R. B., Stewart, W. E., and Lightfoot, E. N., 1960, Transport Phenomena, John Wiley & Sons.

Chima, R. V. and Yokota, J. W., 1990, "Numerical Analysis of Three-Dimensional Viscous Flows in Turbomachinery", AIAA J., Vol.

28, No. 5, pp. 798-806.

Dorney, D. J., Davis, R., and Edwards, D., 1992, "Investigation of Hot Streak Migration and Film Cooling Effects on Heat Transfer in Rotor/Stator Interacting Flows", N00140-88-C-0677 - Report 1, UTRC Report 91-29.

Dring, R. P., Blair, M. F., and Joslyn, H. D., 1980, "An Experimental Investigation of Film Cooling on a Turbine Rotor Blade", Journal of Engineering for Power, Vol. 102, pp. 81-87.

Funazaki, K., Koyabu, E., and Yamawaki, S., 1996, "Effect of Periodic Wake Passing on Film Effectiveness of Inclined Discrete Cooling Holes Around the Leading Edge of a Blunt Body", ASME Paper 96-GT-207.

Goldstein, R. J., 1971, "Film Cooling", Advances in Heat Transfer, Vol. 7, pp. 321-379.

Heidmann, J. D., 1995, "A Numerical Study of the Effect of Wake Passing on Turbine Blade Film Cooling", NASA TM-107077 and AIAA-95-3044.

Heidmann, J. D., 1996, "The Effect of Wake Passing on Turbine Blade Film Cooling", NASA TM-107380 and Ph.D. Dissertation, Case Western Reserve University (1997).

Ito, S., Goldstein, R. J., and Eckert, E. R. G., 1978, "Film Cooling of a Gas Turbine Blade", Journal of Engineering for Power, Vol. 100, pp. 476-481.

Mehendale, A. B., Han, J.-C., Ou, S., and Lee, C. P., 1994, "Unsteady Wake Over a Linear Turbine Blade Cascade With Air and CO_2 Film Injection: Part II - Effect on Film Effectiveness and Heat Transfer Distributions", Journal of Turbomachinery, Vol. 116, pp. 730-737.

O' Brien, J. E. and Capp, S. P., 1989, "Two-Component Phase-Averaged Turbulence Statistics Downstream of a Rotating Spoked-Wheel Wake Generator", Journal of Turbomachinery, Vol. 111, pp. 475-482.

Ou, S., Han, J.-C., Mehendale, A. B., and Lee, C. P., 1994, "Unsteady Wake Over a Linear Turbine Blade Cascade With Air and CO_2 Film Injection: Part I - Effect on Heat Transfer Coefficients", Journal of Turbomachinery, Vol. 116, pp. 721-729.

Rigby, M. J., Johnson, A. B., and Oldfield, M. L. G., 1990, "Gas Turbine Rotor Blade Film Cooling With and Without Simulated NGV Shock Waves and Wakes", ASME Paper 90-GT-78.

Simoneau, R. J., Morehouse, K. A., VanFossen, G. J., and Behning, F. P., 1984, "Effect of a Rotor Wake on Heat Transfer From a Circular Cylinder", NASA TM-83613.

Takeishi, K., Matsuura, M., Aoki, S., and Sato, T., 1990, "An Experimental Study of Heat Transfer and Film Cooling on Low Aspect Ratio Turbine Nozzles", Journal of Turbomachinery, Vol. 112, pp. 477-487.

Takeishi, K., Aoki, S., Sato, T., and Tsukagoshi, K., 1992, "Film Cooling on a Gas Turbine Rotor Blade", Journal of Turbomachinery, Vol. 114, pp. 828-834.

REPORT DOCUMENTATION PAGE

Form Approved
OMB No. 0704-0188

1. AGENCY USE ONLY (*Leave blank*)	2. REPORT DATE	3. REPORT TYPE AND DATES COVERED
	March 1997	Technical Memorandum

4. TITLE AND SUBTITLE

An Experimental Study of the Effect of Wake Passing on Turbine Blade Film Cooling

5. FUNDING NUMBERS

WU–505–62–10

6. AUTHOR(S)

James D. Heidmann, Barbara L. Lucci, and Eli Reshotko

7. PERFORMING ORGANIZATION NAME(S) AND ADDRESS(ES)

National Aeronautics and Space Administration
Lewis Research Center
Cleveland, Ohio 44135–3191

8. PERFORMING ORGANIZATION REPORT NUMBER

E–10671

9. SPONSORING/MONITORING AGENCY NAME(S) AND ADDRESS(ES)

National Aeronautics and Space Administration
Washington, DC 20546–0001

10. SPONSORING/MONITORING AGENCY REPORT NUMBER

NASA TM–107425

11. SUPPLEMENTARY NOTES

Prepared for the 42nd Turbo Expo sponsored by the American Society of Mechanical Engineers, Orlando, Florida, June 2–5, 1997. James D. Heidmann and Barbara L. Lucci, NASA Lewis Research Center; Eli Reshotko, Case Western Reserve University, Cleveland, Ohio 44106. Responsible person, James D. Heidmann, organization code 5820, (216) 433–3604.

12a. DISTRIBUTION/AVAILABILITY STATEMENT

Unclassified - Unlimited
Subject Category 07

This publication is available from the NASA Center for AeroSpace Information, (301) 621–0390.

12b. DISTRIBUTION CODE

13. ABSTRACT ***(Maximum 200 words)***

The effect of wake passing on the showerhead film cooling performance of a turbine blade has been investigated experimentally. The experiments were performed in an annular turbine cascade with an upstream rotating row of cylindrical rods. Nickel thin-film gauges were used to determine local film effectiveness and Nusselt number values for various injectants, blowing ratios, and Strouhal numbers. Results indicated a reduction in film effectiveness with increasing Strouhal number, as well as the expected increase in film effectiveness with blowing ratio. An equation was developed to correlate the span-average film effectiveness data. The primary effect of wake unsteadiness was found to be correlated by a streamwise-constant decrement of 0.094·St. Steady computations were found to be in excellent agreement with experimental Nusselt numbers, but to overpredict experimental film effectiveness values. This is likely due to the inability to match actual hole exit velocity profiles and the absence of a credible turbulence model for film cooling.

14. SUBJECT TERMS

Turbines; Film cooling; Wakes

15. NUMBER OF PAGES

09

16. PRICE CODE

A02

17. SECURITY CLASSIFICATION OF REPORT	18. SECURITY CLASSIFICATION OF THIS PAGE	19. SECURITY CLASSIFICATION OF ABSTRACT	20. LIMITATION OF ABSTRACT
Unclassified	Unclassified	Unclassified	